M. De Lucia
R. De Sabato

Dipartimento di Energetica,
Università degli Studi di Firenze,
Florence, Italy

P. Nava
S. Cioncolini

Nuovo Pignone General Electric,
Florence, Italy

Temperature Measurements in a Heavy Duty Gas Turbine Using Radiation Thermometry Technique: Error Evaluation

This paper describes a technique for the analysis of temperature measurement data obtained by using a radiation thermometer in a heavy duty gas turbine (PGT2 from Nuovo Pignone GE). The main sources of error are shown and analyzed and their influence on measurements and techniques used to correct data read. Success in significant error elimination in acquisition results in a more realistic and correct description of target temperature distribution [DOI: 10.1115/1.1341205]

Introduction

Infrared temperature measurement techniques are used when contact with a hot target is not advisable or even impossible. This is the case, for example, with moving bodies, targets not achievable by traditional instruments, surfaces characterized by such a high temperature as to risk damaging contact sensors or when the same contact with the measuring instrument can modify the target temperature. The advantages in using a radiometric thermometer instead of the traditional contact sensor in gas turbine monitoring are as follows:

- a high level of working frequency (both for the real optic sensor and for the electronic conditioning system);
- a high sensitivity and accuracy of measuring temperature;
- the characteristic of not being an intrusive scanning system (to avoid thermal and fluidynamic interference in turbomachinery flows);
- the possibility, provided by a flexible optic fiber cable, of keeping all the electronic instruments far away from the working area.

On the other hand, there are some drawbacks:

- the need to work with very high optic efficiency;
- the limitation of using the radiation thermometer only in the temperature range for which it was designed;
- a more complex management of the system (the need, for an excellent spatial and temporal resolution, use of uncertainty parameters, limitation and/or control of optic contamination);
- higher cost of this system as compared with traditional ones;
- frequent need for a technician for obtaining efficient measurements.

Measurement Errors. Errors occurring in turbomachinery radiometric scanning are mainly due to the hostile environment in which the instrument must work and this causes the optic contamination of the signal reaching the infrared sensor. The main error sources are:

(a) signal dumping due to the inclination between target surface and radiation thermometer axis;
(b) emitted and reflected radiation coming from hot combustion gas constituting the turbine stage environment;
(c) interference due to transient events;
(d) emitted and reflected radiation coming from the mirror system used for optic signal deviation;
(e) in a GT environment, radiation reaching a sensor is due not only to that emitted by the target, due to its temperature, but also to that reflecting from the surrounding hot areas.

Influence of Target Inclination Angle. Working in perfect environmental conditions, a radiation thermometer can measure the target temperature correctly when its surface is exactly perpendicular to the instrument axis. A target angular inclination causes a signal reduction that, at a certain stage, becomes unacceptable for realistic scanning. So, it is important to determine the exact calibration curve, for each particular radiation thermometer used in measurements, like the one shown in Fig. 1.

As Fig. 1 shows, errors in measuring can be neglected only when working with an inclination lower than 30 deg. Then, it is really important to guarantee this condition or predispose a system able to determine this angle and make an automatic correction of the acquired signal.

Emitted and Reflected Radiation Coming From Enviroment Gas. Combustion gas present in the first stages of turbo engines consists of steam, CO_2, CO, and SO_2, unburned particles and dust. These constituents cause a considerable number of emission, reflection, and scattering phenomena that can be sources of serious temperature measurement errors.

The emission due to a monatomic gas concerns the UV wavelength and only a small area of the infrared region (the one nearest to the visible band).

Symmetrically biatomic molecules (O_2, N_2, etc.) are transparent to infrared rays at low and middle temperatures, and the same happens to the asymmetric ones (CO, NO, etc.) whose emission can be neglected in the radiation thermometer working field.

Triatomic molecules (H_2O, CO_2, SO_2, N_2O, etc.) are, on the other hand, characterized by a strong emission in the infrared region so that their influence must be carefully assessed. This problem could be solved by considering radiative behavior of combustion gases, their composition and temperature but, in the modern GT, concentration of these components can change strongly and rapidly from one area to another. So the best solution is to overcome this problem by using filters able to restrict the working wavelength range to the field in which the influence of hot gas is minimized ($\lambda = 1-1.2\ \mu m$).

Interference due to Transient Events. The main transient events in radiometric scanning of a gas turbine are due to the sight of the flame coming from the combustion chamber and to carbon particles in exhaust gas. The effect of complex transient events is

Contributed by the International Gas Turbine Institute (IGTI) of THE AMERICAN SOCIETY OF MECHANICAL ENGINEERS for publication in the ASME JOURNAL OF ENGINEERING FOR GAS TURBINES AND POWER. Paper presented at the International Gas Turbine and Aeroengine Congress and Exhibition, Indianapolis, IN, 7–10 June 1999; ASME Paper 99-GT-311. Manuscript received by IGTI, March 1999; final revision received by the ASME Headquarters, August 2000. Associate Technical Editor: H. D. Nelson.

PROOF COPY 022101GTP

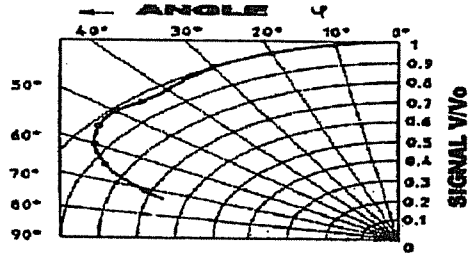

Fig. 1 Signal reduction due to inclination

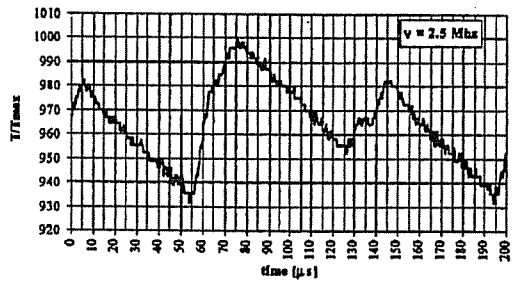

Fig. 3 Temperature measurement at 2.5 MHz (2MW-GT)

generally not such a big problem in heavy duty gas turbines. There is a problem, however, with particles that have not completed their combustion and are dragged from the flow in the first turbine stages. Generally, they are particles with a high volume-surface ratio that, while finishing their oxidation, are like small and strong moving radiation sources whose influence on measurement is significant since they cause temperature over-evaluation (shown by unreasonable and nonperiodic peaks in the output signal). This problem can be totally eliminated by simple data post-processing (i.e., filtering of nonperiodic spikes).

Radiation Emitted and Reflected by Mirror. The optic signal arriving from the target to the radiation thermometer photosensor can be direct or diverted by using one or more mirrors. This technique is used when it is necessary to increase the instrument view area to obtain a complete blade radiometric scanning. Of course, their presence causes some problems in terms of radiation emission and reflection due to the mirrors themselves.

The mirror must be cooled in order to reduce radiation emission as far as possible. Experimental results show that it is sufficient to cool the mirror at temperature at least 100°C less than the target one, to avoid all sensitive influence on measurements. There is also the problem of the constancy of optic mirror characteristics. The experiment, analyzed in following sections, was carried out without using the mirror system.

Experimental Setup. In order to acquire rotor blade temperature distribution, the radiation thermometer was positioned as shown in Fig. 2(*A*). Turbine rotation makes the target move along the blade from TIP to HUB till a point at which the sight radiation thermometer is covered by the next blade passage. By changing instrument inclination, it is possible to move this point as near to or as far away from the HUB as necessary. The instrumentation used was:

(a) radiation thermometer: model R7QB from Land Infrared customized;
(b) spot dimension: 4 mm circular with focal length of 100 mm;
(c) blade area inspected: 16 mm from the TIP (c. 60 percent of the blade).

Experiments were carried out trying to limit the optic contamination reaching the radiation thermometer sensor. These tests were repeated using different sampling rate values to evaluate the influence of a different spatial resolution. In Figs. 3 and 4 test results obtained on the first rotor stage with a sampling rate of 2.5 Mhz (the highest) and 0.1 Mhz (the lowest) are shown.

As can be seen, the use of a higher sampling rate allows a better description of temperature distribution due to the possibility of acquiring the smallest variation in time intervals. On the other hand, it also allows to get more details on the coming radiation. The temperature distribution obtained in this way cannot be considered as representative of the real situation. In fact:

- a turbine stage is a nonisothermal environment so that in target radiative temperature measurement it is necessary to consider the influence of the surroundings;
- the radiation thermometer works using a finite resolution that causes the loss of some information with the consequent signal reduction during scanning.

Radiation Reaching. In a nonisothermal environment, radiation measured by a radiation thermometer is due not only to that actually emitted by the target, due to its temperature, but also to that reflecting from the surrounding hot areas onto the target adding to that measured by radiation thermometer [1–5]. Scientific literature suggests considering the influence of reflected radiation by using a correction coefficient, named apparent emissivity (ε_a), that must be found, on each occasion, experimentally [6,7]:

$$\varepsilon_a = \frac{L_{ex}(\lambda,T)}{L_b(\lambda,T)} = \frac{L_{em}(\lambda,T)+L_r(\lambda,T)}{L_b(\lambda,T)}.$$

So as not to complicate the analysis, a value equal to one is often suggested. However, in this way what is measured is an altered blade temperature distribution, which is often over-valued. For this reason, the radiative model suggested by De Lucia and Lanfranchi in 1992 [8], and subsequently upgraded by De Lucia and Masotti in 1994 [9], was preferred. This model uses the calculation of view factors between the different surfaces in which the geometric problem is resolved and allows exact calculation of the value of apparent emissivity for each blade point. In this way, it is possible to process the outgoing target radiation, the one measured by the sensor, in order to determine the radiation that a

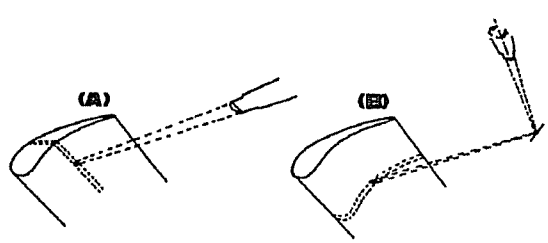

Fig. 2 Comparation between views without and with mirrors

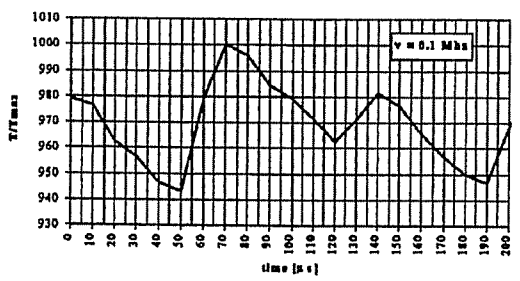

Fig. 4 Temperature measurement at 0.1 MHz (2MW-GT)

PROOF COPY 022101GTP

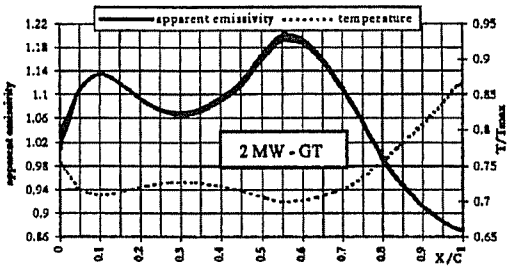

Fig. 5 Apparent emissivity band (rotor blade)

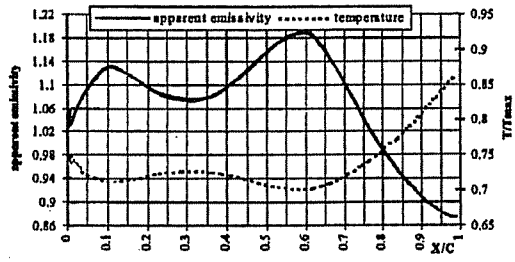

Fig. 7 Apparent emissivity for fictitious GT

black body would emit at the same target temperature. By inverting Planck's law [10,11], it is then possible to evaluate the real target temperature.

In the following, Fig. 5 apparent emissivity distribution is shown, with regard to the pressure side of a first turbine stage rotor blade, and the consequent dimensionless temperature distribution against the target position on the blade (seen as a percentage of the axial chord).

It can be seen that the apparent emissivity distribution is approximately opposed to the temperature distribution so that the higher the temperature the lower the apparent emissivity determined at the same point.

Apparent emissivity values, for first rotor stage, range from a minimum of 0.87, on the suction side, to a maximum of 1.2 on the pressure side (from 0.8 to 2 for the stator blade). So the usual hypothesis of considering a value of 1 becomes an acceptable approximation only when a high level of precision for measurements is unnecessary since errors on ϵ_a evaluation can reach values of 20 percent (even 100 percent for the stator blade).

We also need to consider that apparent emissivity is a function of temperature distribution but also of geometric disposition of all the target surfaces. To consider the influence of geometry, the calculation was repeated in ten different positions between rotor and stator. This continuous changing of the geometry due to the turbine rotation causes a periodic variation of apparent emissivity calculated. So, this is a function of time as well as of spatial position. However, looking at the narrow band (see Fig. 5) in which the apparent emissivity values are positioned, it is possible to realized there is not a big error in considering a mean value of the ten positions.

In terms of temperature, the exact calculation of apparent emissivity, instead of using a value of one, allows avoidance of overevaluation of temperature distribution (15°C–45°C) far too high to be accepted.

To confirm these results, the same analysis was carried out for a new generation turbine characterized by a geometry and a cooling system very different from the previously seen GT. Even in this case (see Fig. 6), the apparent emissivity distribution is opposite to the temperature distribution:

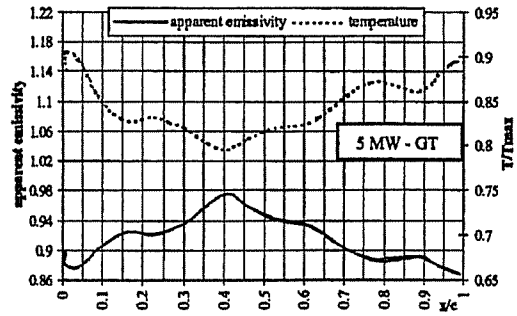

Fig. 6 Apparent emissivity (rotor blade)

And here the temperature error due to considering the mean value of ε_a instead of its temporal one is minute (less than 0.3 percent versus 0.2 percent of the previous case).

Influence of Geometry and Temperature Distribution on Determining of ε_a

To understand better the importance of temperature distribution and system geometry with regard to apparent emissivity calculation, the same process shown before was repeated for a fictitious turbine characterized by the same geometry of that of a latest generation machine (5 MW-GT) and the temperature distribution of the first one examined in this paper (2 MW-GT). The results obtained (see Fig. 7) are only indicative and cannot demonstrate anything but are of considerable interest.

They show that apparent emissivity distribution is similar to the one just found for the rotor blade of the first turbomachine analyzed (see Fig. 5). This means that theoretical temperature distribution is the main parameter influencing apparent emissivity value while much less remarkable is the effect of view factors (and then the influence of geometry).

The Problem of Finite Resolution

During data aquisition, the radiation thermometer can read temperature values along the blade side due to its rotation movement. The view is only possible up to the moment at which the TIP of the following blade covers the previous one (see Fig. 8).

At the passage between a blade and the following one, when the radiation thermometer sees two very different temperature distribution (high temperature for the blade TIP and low temperature for HUB), there is a major error in aquisition. The radiation thermometer spot (the area seen by instrument focal system) has a finite dimension (it is not really a point as theory supposes) and a particular shape. The consequence is that the temperature acquired is not the real one relative to the point seen by the instrument but an average value of the temperature of all the blade points in the radiation thermometer spot area. So, during blade passage, the measured temperature is a value that is not representative of any real situation.

To understand the influence of spot shape, it is possible to see the variation of temperature measurement obtained by a radiation

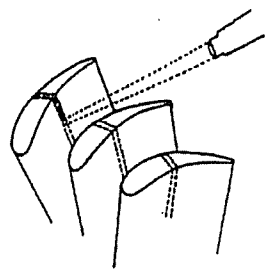

Fig. 8 Scanning blade measurement (along blade height)

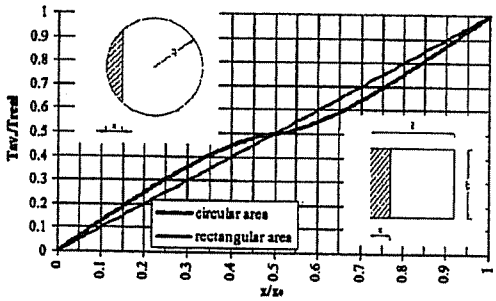

Fig. 9 Influence of spot shape

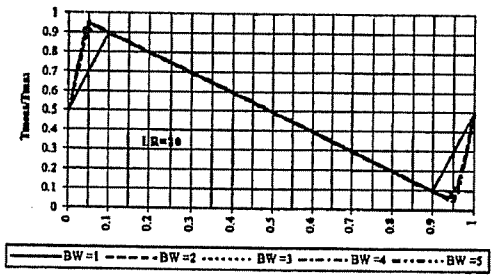

Fig. 10 Signal reduction for circular spot varying BW

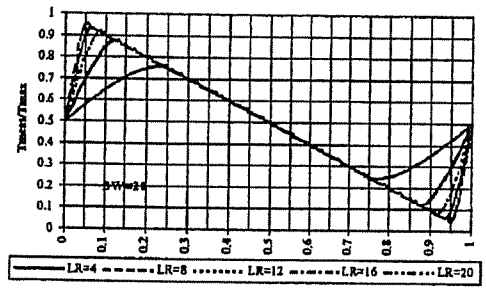

Fig. 11 Signal reduction for circular spot varying LR

thermometer that scans an isothermal surface, against the percentage of area seen by the instrument when a rectangular or a circular spot is used. Results are reported in dimensionless terms in Fig. 9.

As can be seen, rectangular spot behavior is linear while that of the circular spot is different, and more complex (the latter is the most common). Apart from spot shape, there are two other really important parameters: the spot dimension and the signal rate sampling that cause an alteration of measurement during blade passage. The problem of correction of this kind of error was faced by considering a sawtooth signal and simulating its scanning by radiation thermometer. The main parameters are the value of LR (the ratio between the blade visible length l and the radius R_{spot} of the circular spot) considering the geometric dimensions of the problem and the value of BW (ratio between the rate sampling and the machinary rotation frequency) considering the accuracy by which the signal is scanned. Naming the abscissa determining the spot position on blade z, the dimensionless equations characterizing instrument behavior (circular spot) in the regions in which there are the three different temperature distributions are as follows:

$$0 \le z \le R_{spot}$$

$$\frac{T_{max}(z)}{T_{max}} = \left(1-\frac{z}{l}\right) + \frac{1}{\pi}\cdot\left(\frac{z}{R_{spot}}\right)\cdot\sqrt{1-\left(\frac{z}{R_{spot}}\right)^2} + \frac{1}{\pi}\arcsin\left(\frac{z}{R_{spot}}\right) - \frac{1}{2}, \tag{1}$$

$$R_{spot} \le z \le l - R_{spot}, \quad \frac{T_{meas}(z)}{T_{max}} = 1 - \frac{z}{l}, \tag{2}$$

$$l - R_{spot} \le z \le l$$

$$\frac{T_{meas}(z)}{T_{max}} = \left(1-\frac{z}{l}\right) + \frac{1}{2} - \frac{1}{\pi}\cdot\left(\frac{l}{R_{spot}} - \frac{z}{R_{spot}}\right) \cdot\sqrt{1-\left(\frac{l}{R_{spot}} - \frac{z}{R_{spot}}\right)^2} - \frac{1}{\pi}\cdot\arcsin\left(\frac{l}{R_{spot}} - \frac{z}{R_{spot}}\right). \tag{3}$$

Since the measurement of z abscissa cannot be carried out continuously but in an interrupted manner, it is possible to write the discrete space covered at instant i as $z_i = z_{i1} + dz$, $dz = L/BW$ being the incremental spatial step made by the blade (and measured in a direction perpendicular to that of the radiation thermometer axis) between two following readings. Now it is possible to write the following ratios:

$$\frac{l}{R_{spot}} = LR; \quad \frac{z}{l} = \frac{i\cdot dz}{l} = i\cdot\frac{1}{BW};$$

$$\frac{z}{R_{spot}} = \frac{i\cdot dz}{R_{spot}} = \cdot\frac{i\cdot dz}{L}\cdot\frac{l}{R_{spot}} = i\cdot\frac{1}{BW}\cdot LR.$$

In this way, all the previous expressions can be written as a function only of LR and BW. Then, changing the value of these two ratios, two curve families were generated to show their real influence in data aquisition.

As can be seen in Fig. 10, for a fixed value of LR, the greater the sampling rate, in respect of rotation frequency, the lower the reduction of the signal measured in respect of the real one. On the other hand, the lower the sampling rate the greater the loss of information so that the accuracy in describing temperature distribution is lower (it is possible to have a reduction even greater than 10 percent; see Fig. 10 BW=1).

In our tests, sampling rate changed from 0.1 Mhz to 2.5 Mhz while the rotation speed was 22,500 rpm. So, BW changes from 266 to 6667 with a consequent negligible signal reduction.

The LR ratio, in our case, has a value of 10 so that, considering the worst values for BW, it is even possible to have a reduction greater than 10 percent, as is shown in Fig. 11.

Data Analyzing Model

Temperature measurement is the result of an integration on spot area of the radiation really emitted by the target. Information loss concerning temperature distribution in spaces smaller than the spot diameter causes the impossibility of rebuilding the real signal on the basis of acquired data. To overcome this problem we built up a theoretical model of temperature distribution, simulating realistically its scanning (same values for LR and BW) to obtain a corrupted signal and compare it with the signal acquired by using a radiation thermometer on the turbomachinery. The greater or lesser coincidence between the corrupted theoretical signal and the real measurement gives some information about the goodness of the initial theoretical model. Since incorrect behavior of the cooling system of a blade, superficial irregularity, or local oxidation of some part of another blade can justify a different temperature distribution between blades, obtaining any signal periodicity, i.e., an identical distribution on every blade, cannot be contemplated. In this way, the theoretical model must be built up starting from the signal measured and using an iterative model to search for the best congruence between the corrupted and measured ones.

Many theoretical models were built up. Those the authors consider the best for analysis are presented here:

PROOF COPY 022101GTP

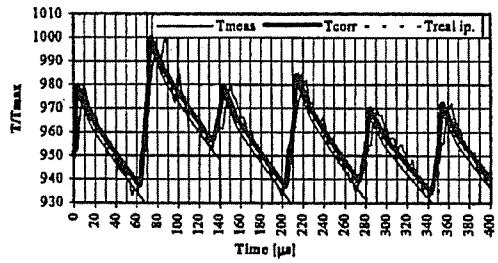

Fig. 12 Simple sawtooth model

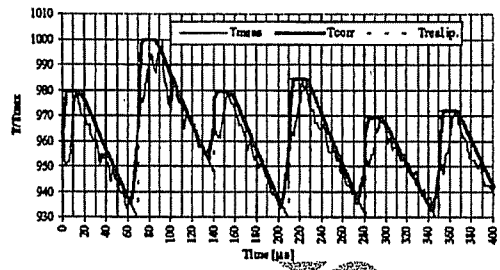

Fig. 13 Trapezoidal model

(a) simple sawtooth model (see Fig. 12);
(b) trapezoidal model (see Fig. 13);
(c) modified trapezoidal model (see Fig. 14).

In Fig. 15, the application can be seen of each of these models to the same temperature data series. In the following graphs, the experimental measured signal (T_{meas}), the theoretical model adopted ($T_{real\ ip.}$), and the corrupted one (T_{corr} obtained integrating the theoretical signal on the spot area) are shown.

The first model seems to fit well the acquired signal; the correspondent RMS value, that is the evaluation parameter adopted to find the best theoretical model is 0.085. The second case seems to be the worst; here is an increase of RMS that reaches a value of 0.104. The last model is closest to the signal measured; RMS value is 0.06, the lowest, so that this is the model used for data analysis.

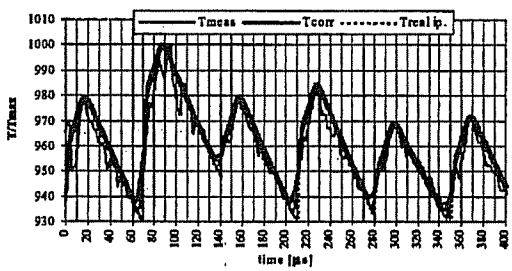

Fig. 14 Modified trapezoidal model

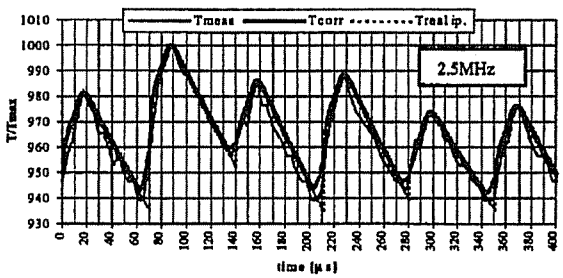

Fig. 15 2MW GT temperature measurement

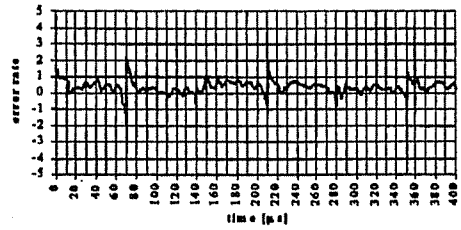

Fig. 16 Temperature error ($T_{meas}-T_{corr}$)

Experimental Results

Analysis was carried out on different data series obtaining in each case coherent and comparable results. Thus only one of them is shown here.

Difference between corrupted signal and acquired one is always less than 1 percent.

After defining the model, the error due to the finite resolution with which the radiation thermometer works can be estimated.

As shown in Fig. 16, errors become noticeable only during blade passage. In terms of temperature, the maximum error is about 2 percent (only in few cases is it more than 3 percent).

Error Evaluation

The overall error without any correction can be evaluated as follows:

- First correction seeks to avoid the effect of finite resolution in temperature measurement. Naming $T_{fin.res.}$ the temperature obtained on the basis of this correction and $e_{fin.res.}$ the percentage difference between $T_{fin.res.}$ and the measured temperature, it is possible to write this expression:

$$e_{fin.res.}=\frac{T_{fin.res.}-T_{meas}}{T_{fin.res.}}\Rightarrow T_{fin.res.}=\frac{T_{meas}}{(1-e_{fin.res.})}.$$

- Then the correction due to apparent emissivity must be introduced in order to consider the not so ideal environment. Defining the intermediate temperature as radiance temperature T_λ obtained when errors due to the physics phenomena and imperfections in radiation thermometer working are eliminated (in this case $T_\lambda=T_{fin.res.}$), we can define a new error:

$$e_{rad}=\frac{T_{real}-T_\lambda}{T_{real}}$$

so that we have

$$T_{real}=\frac{T_\lambda}{1-e_{rad}}=\frac{T_{meas}}{(1-e_{rad})\cdot(1-e_{fin.res.})}.$$

Temperature distribution against the generic T_{meas} measured, without considering any correction (T_{meas}), considering the finite resolution of radiation thermometer ($T_{fin.res.}$) and in the case in which we consider even the effect of apparent emissivity (T_{real}), are all plotted in Fig. 17.

In terms of temperature, these errors correspond to ΔT of 30°C–50°C that means an error up to 6 percent.

As can be seen, these two corrections have opposite effect: the first one causes a temperature distribution increase because of the elimination of reduction due to finite resolution; on the other hand, the second causes a decrease in temperature, owing to the elimination of signal over-evaluation due to the contribution of apparent emissivity (reflected radiation coming from surroundings).

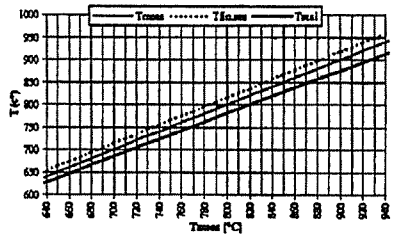

Fig. 17 Temperature correction vs T_{meas}

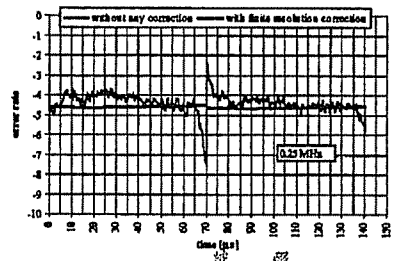

Fig. 18 Percentage error rate at 2.5 MHz

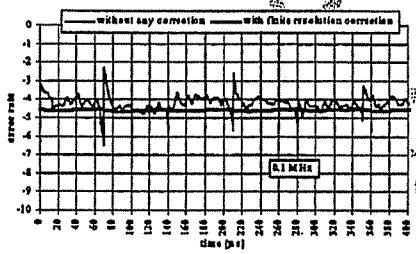

Fig. 19 Percentage error rate at 0.1 MHz

Now it is possible to see, for data obtained by sampling with the maximum rate (2.5 Mhz), which is the real error without considering any correction or considering only the effect of finite resolution.

As can be seen in Fig. 18, not using any correction causes an error whose peaks are even greater than 7 percent (during blade passage) and whose average value is about 4 percent–5 percent.

The same operation can be repeated for the lower sampling rate (0.1 Mhz); see Fig. 19.

Here, again, not using any temperature correction causes an error whose peaks occur during blade passage while their average value is about 4 percent–5 percent.

Conclusions

An extension of the data correction model would foresee the improvement of a tridimensional model to better determine view factors (the model used is bidimensional) to consider the ever more complex geometry of modern turbomachinery. This way of working seems to be far better than that followed and proposed by scientific literature up to now (in which corrections are absent or are extremely approximate, e.g., considering $\varepsilon_a = 1$).

In this analysis, correction due to surface inclination is not considered. So there is another error whose value can reach about 3 percent–4 percent.

However, by using the proposed correction it is possible to avoid errors, in temperature evaluation, whose average value for working temperature up to 950°C is about 40°C with peaks of 65°C, in this way allowing better system monitoring and a more realistic description of blade temperature distribution.

Future developments could regard the definition of a better theoretical model in order to improve fitting to obtain the best possible final result.

Acknowledgments

The authors are grateful to the NuovoPignone experimental staff for their help in carrying out the experimental program and to Professor Ennio Carnevale for his invaluable support.

Nomenclature

BW = sampling rate to machinery rotation ratio
D, R = diameter and radius
E = error
L = radiance W m^{-2} sr^{-1} μm^{-1}
l = visible blade length
LR = blade visible length to radius spot ratio
T = temperature
z = abscissa of spot position on blade
ε = emissivity
λ = wavelength μm

Subscripts

a = apparent
av = average
b = blackbody
corr = corrupted
em = emitted due the temperature surface
ex = exitent
fin.res = finite resolution
meas = measured
r = reflected
real.hp = theoretical hypothesis

References

[1] Beynon, T. G. R., 1981, "Turbine Pyrometry-An Equipment Manufacturer's Viewpoint," ASME Paper 81-GT-136.
[2] Beynon, T. G. R., 1982, "Infrared Radiation Thermometry Applied to the Development and Control of Gas Turbine Engines," *Proceedings, International Conference on Infrared Technology*, Butterworth Scientific, Ltd., Sevenoaks, U.K., pp. 3–16.
[3] DeWitt, P. D., and Incropera, F. P., 1988, "Physics of Thermal Radiation," *Theory and Practice of Radiation Thermometry*, edited by P. D. DeWitt and G. Nutter, Wiley, New York, NY, pp. 21–89.
[4] Douglas, J., 1980, "High-Speed Turbine Pyrometry in Extreme Environments," Proceedings, New Orleans Gas Turbine Conference, ASME, New York, NY, pp. 335–343.
[5] Kirby, P. J., Zachary, R. E., and Ruiz, F., 1986, "Infrared Thermometry for Control and Monitoring of Industrial Gas Turbines," Proceedings, International Gas Turbine Conference and Exhibit, Duesseldorf, Germany, ASME Paper 86-GT-267.
[6] Schulemberg, T., and Bals, H., 1987, "Blade Temperature Measurements of Model V84.2 100 MW/60 Hz Gas Turbine," Proceedings, International Gas Turbine Conference and Exhibit, Anaheim, CA, ASME Paper 87-GT-135.
[7] Scotto, M. J., and Eismeier, M. E., 1980, "High-Speed Noncontacting Instrumentation for Jet Engine Testing," ASME J. Eng. Power, 102, pp. 912–917.
[8] De Lucia, M., and Lanfranchi, C., 1992, "An Infrared Pyrometry System for Monitoring Gas Turbine Blades: Development of a Computer Model and Experimental Results," 1992, IGTI-92, Paper No. 92-GT-80. ASME, Journal of Engineering for Gas Turbines and Power, January 1994, Vol. 116, pp. 172–177.
[9] DeLucia, M., and Masotti, G., 1994, "A Multimeasurement Infrared Pyrometry System for Determining Temperature Distribution in Gas Turbines," IGTI 94, Paper No. 94-GT-39, ASME, Journal of Engineering for Gas Turbines and Power, April 1995, Vol. 117, pp. 341–346.
[10] Love, T. J., 1988, "Environmental Effects on Radiation Thermometry," *Theory and Practice of Radiation Thermometry*, edited by P. D. DeWitt and G. Nutter, Wiley, New York, NY, pp. 189–229.
[11] Ono, A., 1988, "Methods for Reducing Emissivity Effects," *Theory and Practice of Radiation Thermometry*, edited by P. D. DeWitt and G. Nutter, Wiley, New York, NY, pp. 565–623.

PROOF COPY 022101GTP